BII-3

THE STRENGTH AND TOUGHNESS OF DYNAMICALLY STRAIN AGED ALLOY STEELS

V.F. Zackay*, W.W. Gerberich*†, R. Busch* and E.R. Parker*

ABSTRACT

The response of alloy steels to dynamic strain aging in both quenched and tempered and ausformed conditions were investigated. Strength, ductility, and toughness were measured as a function of straining and tempering temperatures. Structural observations were made on the strained and unstrained steels.

By appropriate choice of strain and tempering temperatures, the strength of quenched and tempered steels was increased by about 40,000 psi, i.e., to the base strength of the ausform steels. The strength of the ausform steels was increased by about the same amount, suggesting that the strengthening effects are additive.

In the ausform steels, yield strengths of 270,000 psi were achieved by dynamic strain aging with a reliability ratio (K_c/σ_{ys}) of one. Since the slope of K_c/σ_{ys} vs σ_{ys} is small, it is suggested that this process may be used to attain yield strengths of 300,000 psi with exceptional toughness.

* Inorganic Materials Research Division, Lawrence Radiation Laboratory, and Department of Mineral Technology, College of Engineering, University of California, Berkeley, California

† Aerojet-General Corporation, Sacramento, California

V.F. Zackay, W.W. Gerberich, R. Busch and E.R. Parker

INTRODUCTION

A major concern of metallurgists is that of obtaining increased strength with a margin of reliability. Until about 1960, brittle fracture in steel, aluminum, and titanium alloys was a problem whenever the yield strength-to-density ratio exceeded 750,000 inches.[1,2]

More recently, several titanium alloys with adequate toughness have been developed with strength-to-density ratios approaching 1,000,000 inches. For steels to be competitive with such materials, yield strengths above 250,000 psi are necessary. Attempts to obtain both this strength and toughness in steels have, in general, been unsuccessful. Developments that have improved the stature of high-strength steels are the high nickel alloys and certain thermal-mechanical treatments. In the first, the maraging steels[3] (18 Ni-9Co-4Mo) and the 9Ni-4Co carbon steels have yield strengths above 240 ksi with acceptable toughness. In the thermal-mechanical category, ausforming is probably the most widely known process and has been shown to improve the strength-toughness relationship.[4] Similarly, cold-working austenitic stainless steels[5] in the metastable region (-200°C) and various thermal-mechanical treatments of bainites and martensites hold some promise.

Perhaps the greatest single improvement was made by utilizing low-carbon modified steels in the ausform process.[4] For example, fracture toughness to yield strength ratios (K_c/σ_{ys}) greater than unity have been attained in a 0.25 carbon modified 5Cr die steel with yield strengths of 250,000 psi and ultimate strengths of 300,000 psi. There are reasons to believe, however, that the structure of this material is not characteristic of ausformed steels.[6] Other low carbon steels, such as 5M21 (a 3Ni-3Mo die steel) and Hy-Tuf (a 1.8Ni-1Cr-0.5Mo steel), have shown similar K_c/σ_{ys} ratios with yield strengths on the order of 240,000 psi.[7] In the latter materials, however, there seemed to be a rapid loss in toughness with yield strengths much greater than this.

It was the purpose of this investigation to apply dynamic strain aging to initially tough materials in order to obtain useful strength-toughness combinations in the ultra-high strength regime. Dynamic strain aging as defined in this investigation is a process where the strain is applied at an elevated temperature. The reason for utilizing this process was two-fold:

(a) Prior information on dynamically strain aged H-11 (5Cr-0.40 carbon die steel) indicated that large yield strength increases could be obtained without any loss of ductility.[8] Stable load-elongation curves were obtained as opposed to the yield instability associated with conventional strain aging.[9]

(b) As indicated above, prior information on the fracture characteristics of ausform low carbon steels indicated that good toughness could be realized at the 240,000 psi yield strength level.

It was anticipated that a combined thermal-mechanical treatment could result in even greater yield strengths with excellent toughness. From this background, three low alloy steels with carbon levels ranging from 0.19 to

0.26 percent were chosen, i.e., 5M21, Hy-Tuf and low carbon D6aC. The first two were selected because of prior success obtained with them in the ausform condition and the latter because of its intermediate amount of alloying elements and its relatively good strength-toughness relationship in the higher carbon variety.[4] An added advantage is that Hy-Tuf, D6aC, and 5M21 have low, medium, and high hardenability, respectively, which determines the usable section size in practical applications.

MATERIALS AND PROCESSING

The materials for this investigation were supplied by the Crucible Steel Company in the form of 1/16" thick sheets, both in the ausform and quenched and tempered conditions. The compositions are shown in Table I. The austenitizing temperatures were the same for both conditions: 900°C for Hy-Tuf and D6aC, and 1040°C for 5M21. The ausform steels, reduced 50% by rolling, were deformed at 595°C, 565°C, and 620°C for Hy-Tuf, D6aC, and 5M21, respectively, and oil quenched. The conventionally heat treated sheets were oil quenched directly from the austenitizing temperature. All steels were tempered twice for two hours at 205°C. The sheets were strained at selected temperatures by pack rolling in order to achieve uniform strain. The actual temperature during strain, as determined by a contact pyrometer, was estimated to be within ± 10°C of the reported value. Measured reductions in thickness were 2-1/2 ± 1% for the ausformed steels and 6 ± 1% for the quenched and tempered steels.

PROCEDURES

Longitudinal tensile and Charpy specimens were cut from the sheets and tempered before final grinding. Tensile tests were performed at room temperature on a 12,000 lb Universal testing machine at a strain rate of .005/min. to yield, and .050/min. to fracture.

For screening purposes, pre-cracked Charpy specimens were tested for each condition. From these and the tensile data, conditions for "wide-plate" fracture toughness tests were selected. In preparing the pre-cracked Charpy specimens, a somewhat sharper than standard V-notch was milled so that the root radius was about 0.005 inches. This was subsequently fatigue-cracked in a three-point bending device that propagated the crack perpendicular to the original front. After extending the fatigue crack approximately 30 mils, the specimens were tested on a subsize Charpy machine with a capacity of 24 ft-lbs. The results are expressed as energy per unit fracture area where the fracture area is the specimen area minus the notched and fatigue-cracked areas. These areas were measured with aid of a low power binocular microscope with a filar eyepiece.

For the wide-plate tests, nominal 5" × 16" pieces were processed to the desired conditions. All edges were subsequently ground to ensure parallelism. After the specimens were machined in accordance with Fig. 1 of the Appendix, a crack was extended about 50 mils at both ends of the machined slot by cantilever bending. This resulted in wing-type fatigue cracks extending in from each surface until they overlapped. To ensure a valid test, high strength doublers were welded on both sides of the specimen to prevent lateral buckling and yielding in the grips.

A pin and clevis arrangement in a Universal testing machine was utilized which loaded specimens at about 5000 lbs./min. Two methods were utilized to measure the slow crack propagation. First, the ink method[1] was used in conjunction with the standard ASTM analysis for evaluating K_c from,

$$K_c^2 = \sigma_o^2 \, W \tan \left[\frac{\pi a}{W} + \frac{K_c^2}{2W\sigma_{ys}^2}\right] \qquad (1)$$

where σ_o is the applied stress at fracture, σ_{ys} is the yield strength, W is the plate width, and a is the half-crack length at instability. Secondly, a calibrated displacement gage was added and a load-displacement curve was recorded for each test. The gage points were set inside the center-slot so that a zero gage-length set-up was obtained. As the crack extended, the reduced effective modulus gave a measure of the crack length. The secant modulus at fracture was compared to reduced moduli previously obtained during calibration runs on specimens with known crack lengths. Thus, the apparent crack length at instability was determined. It must be emphasized that this is an apparent crack length since the plastic zone developed at the crack tip also reduces the effective modulus. Fracture toughness values were determined from the apparent crack lengths (a') estimated in this manner according to,

$$K_c^2 = \sigma_o^2 \left[W \tan \frac{\pi a'}{W}\right]. \qquad (2)$$

In conjunction with mechanical tests, light and electron microscopy were utilized. Carbide extraction replicas were prepared by standard techniques. For transmission microscopy a limited number of specimens were ground to 0.015" and then chemically polished in a phosphoric acid-hydrogen peroxide solution to 0.005". Thin foils were then obtained by electro-polishing in a 10% perchloric acid, 90% glacial acetic acid solution and examined in an Hitachi HU-11A electron microscope.

EXPERIMENTAL RESULTS AND DISCUSSION

The processing conditions used in this investigation significantly affected the shape of the stress-strain curve, the strength and ductility, the toughness, and the structure of the steels studied. These topics will be discussed in this order.

1. The Influence of Processing on the Shape of the Stress-Strain Curve

The three types of stress-strain curves encountered as a result of the various processing conditions employed are shown schematically in Fig. 1. The large majority of the stress-strain curves were of the conventional kind as shown in (a). In this type, hereafter called Type I, there is a positive slope at the yield point indicative of work hardening, which continues for large strains beyond the yield point. In the second type (Type II) there is a similar overall shape but work hardening occurs over a limited strain ($< 1\%$), as shown in (b). This type of curve was observed only in the dynamically strain aged ausform Hy-Tuf steel. The

third type of curve (Type III) is that typical of room temperature strain aging wherein the slope of the stress-strain curve is negative immediately beyond the yield, as shown in (c). Three such curves were seen in the dynamically strain aged ausform D6aC steel. Several similarly processed specimens of this steel fractured in a brittle manner at very small strains. The limited degree of work hardening, the plastic instability, and the brittleness observed in several of these specimens of the low and medium hardenability steels may be partly related to the ferrite formed during the ausform processing. All stress-strain curves in the quenched and tempered steels were of Type I. A tabulation of all mechanical properties is given in Table I of the Appendix.

2. The Effect of Dynamic Strain Aging on Strength and Ductility

Considering the quenched and tempered steels first, the room temperature yield strength as a function of strain temperature for several tempering temperatures is shown in Fig. 2. The variation of yield strength with temperature of the control specimens, i.e., those heated to the strain temperature but not strained, is also shown. These specimens were simply double tempered. The effect of tempering temperature on the control specimens up to the highest tempering temperature (375°C) was relatively small. However, both the strain temperature and the tempering temperature significantly influenced the yield strength of the dynamically strained specimens.

An average increase of nearly 40,000 psi (for the combination of the higher strain temperatures and the lower tempering temperatures) was observed for the Hy-Tuf and D6aC steels. Also, at a given strain temperature, variations of 10,000 to 20,000 psi were noted within the spread of the tempering temperatures used. The dependence of the yield strength on strain temperature for 5M21 steel, Fig. 2, was different from that of the other two steels in that the strength reached a maximum at an intermediate temperature and dropped off sharply at higher temperatures somewhat akin to "over-tempering" in conventionally treated steels. This steel is the only one of the three that exhibits a secondary hardening peak (550°C) when conventionally heat treated.

In the original design of these experiments, it was intended that all steels be strained two percent at temperature. Inadvertantly, however, the quenched and tempered steels were strained six percent. The influence of this large amount of strain can be seen in Table I of the Appendix. The decrease in room temperature ductility is surprisingly small, e.g., about two percent in elongation for Hy-Tuf and less for the other steels. In several instances, especially at the lower strain temperatures, there was no loss in room temperature ductility. As noted previously, all stress-strain curves of the dynamically strained, quenched, and tempered steels were stable, i.e., of Type I.

The response of the ausform steels to dynamic strain aging was similar in that the yield strength was increased, on the average, about 40,000 psi, as shown in Fig. 3. The yield strength of ausform steels, however, was more sensitive to the straining conditions. The yield strength of D6aC fell to a low level above a strain temperature of 300°C. The effect of tempering temperature on the strength at a given strain temperature is

similar to that of the quenched and tempered steels, viz. a spread of 10,000 to 20,000 psi within the range employed. The ductility of the dynamically strain aged ausform steels showed an even greater sensitivity to strain conditions than did the yield strength. The loss was greatest for Hy-Tuf and least for 5M21, as shown in Table I of the Appendix.

A composite figure showing the strength of quenched and tempered and ausform Hy-Tuf in the strained and unstrained condition is shown in Fig. 4. Base strengths for the quenched and tempered and ausform steel are indicated. The effectiveness of dynamic strain aging as a strengthening mechanism is clearly evident in that both the quenched and tempered and ausform steels exhibited in an increase of about 40,000 psi. This approximately constant increase, independent of initial structure, suggests that the strengthening effects involved in dynamic strain aging and ausforming are additive. Even more significantly, for several conditions, the strength of the strain aged quenched and tempered steels was raised to that of the ausform base strength. This equivalence exists in both Hy-Tuf and D6aC. The strength of the strain aged ausform steels was about 80,000 psi greater than that of the quenched and tempered steels. For certain conditions in all three steels this difference was as high as 100,000 psi.

3. The Effect of Dynamic Strain Aging on Toughness

a. Pre-Cracked Charpy Tests

The toughness of the quenched and tempered steels, as determined by impact testing of pre-cracked Charpy bars, is shown in Fig. 5 as a function of strain temperature. The effect of tempering temperature at a given strain temperature is not shown since the scatter in the toughness measurements was greater than that occasioned by the variation in tempering temperature. The toughness curves represent an average of the values determined at each strain temperature.

Dynamic strain aging decreased the toughness of the quenched and tempered steels, particularly at the higher strain temperatures. The toughness is also decreased somewhat by tempering in the unstrained condition. Taking into account the scatter in the data for the strained and unstrained conditions, there is considerable overlap over a wide range of strain temperatures for Hy-Tuf. The generally high level of toughness observed (in both conditions) for all three steels is consistent with values previously reported in the literature for low carbon quenched and tempered alloy steels.[10]

The toughness of the ausform steels is lower, in both the strained and unstrained condition, than that of the quenched and tempered steels, as shown in Fig. 6. Strain aging decreases the toughness for all three ausform steels, particularly at the lower strain temperatures. At higher strain temperatures the toughness of both conditions is (within the scatter) about the same.

The response of Hy-Tuf to dynamic strain aging for both the quenched and tempered and the ausform states is shown in Fig. 7. The base properties for the unstrained conditions are indicated by dashed lines. The toughness of the strain aged quenched and tempered steel is clearly superior to that

of the ausform steel either strained or unstrained but decreases sharply with increasing strain temperature until it becomes equal to that of the ausform steel at a high strain temperature. This is somewhat unexpected since there is not a corresponding change of strength. Perhaps the dynamic strain aging of the quenched and tempered steel enhances brittleness in the high temperature regime while it has no effect on the ausformed condition. The behavior of both ausform and quenched and tempered D6aC and 5M21 steels is similar in nature to that of Hy-Tuf.

b. Wide Plate Tests

Orner and Hartbower[11] have shown that pre-cracked Charpy tests could be correlated to wide plate fracture toughness tests. They obtained a linear correlation of the two tests on a wide variety of medium-carbon, low-alloy steels as well as non-ferrous alloys. However, since there was a scatter of 400 in-lbs./in^2 for their correlation and the range for those materials having a yield strength over 220,000 psi was less than 500 in-lbs./in^2, it was considered desirable to make some wide plate tests to verify the actual energy release rate. All of the data from the wide plate tests are shown in Table II of the Appendix. It is seen that in all cases the fracture toughness results obtained from the displacement gage analysis are greater than the ASTM result. This indicates that the currently used plastic zone size correction underestimates the toughness, as has been pointed out in a number of recent investigations.[2,12,13] The more conservative value of K_c will be used here as this is the one generally reported. In considering the energy absorption characteristics of a material, the fracture toughness or energy release rate parameter is of significance. However, in terms of a critical crack length and hence, reliability,[4] the fracture resistance ratio, K_c/σ_{ys}, is more meaningful. Both parameters will be discussed. It should be noted that wide plate tests were made only on the ausform steels.

Dynamic strain aging increased the yield strength of 5M21 by 55,000 psi and increased the K_c value by 39 ksi-in.$^{1/2}$. For the unstrained material, the K_c/σ_{ys} ratio was 1.07 while that for the strained material the ratio only decreased slightly to 0.99. Similarly, in the D6aC steel, a 43,000 psi yield strength increase was accompanied by a 37 ksi-in.$^{1/2}$ increase in toughness. This resulted in K_c/σ_{ys} ratios of 1.06 for the unstrained condition and 1.03 for the strained one. Again, the reliability was maintained. Finally, for the Hy-Tuf alloy, increases in yield and toughness were 52,000 psi and 25 ksi-in.$^{1/2}$, respectively, while the fracture resistance ratios were 1.11 and 0.99, respectively. It should be emphasized that a K_c/σ_{ys} ratio of about one for a 270,000 psi yield strength material is exceptional. To illustrate the maintained reliability with increasing yield, the example of a pressure vessel bursting at a membrane stress equal to the yield strength is taken. In this instance, the critical crack length, 2a, for failure at this stress would be about 0.185 inches for the low strength and 0.159 inches for the high strength condition. For the thickness of material we are considering, both of these are very large cracks and could easily be avoided by inspection.

A compilation of the data[2] on conventional quench and temper steels and the best commercially available ultra-high strength steels are shown in Fig. 8. A reliability plot of K_c/σ_{ys} versus the yield strength is

shown with the data of this investigation superimposed. Two points are immediately apparent: (1) that above 250,000 psi yield the strength-toughness combination of the dynamically strain-aged steels is superior to that of the best steels developed to date; (2) that the slope of the curve is small, suggesting that high toughness might be maintained to strength levels as high as 300,000 psi.

Of the materials with yield strengths greater than 247,000 psi, there were four with Type II and III curves and four with a Type I stress-strain curve. For the former, the average yield strength was 268,000 psi and the average K_c was 259 ksi-in.$^{1/2}$, while for the latter the average values were 254,000 psi and 247 ksi-in.$^{1/2}$. Thus, within these experimental conditions, the reliability factor, K_c/σ_{ys}, of the materials showing a limited work hardening range or an actual instability is equal to that of the materials showing stable behavior.

c. Comparison of Toughness Tests

To compare the pre-cracked Charpy results to the wide plate tests, W/A values from the Charpy tests are plotted versus the corresponding in-lb./in.^{2} values (obtained from $G_c = K_c^2/E$) in Fig. 9. There is no correlation of the type observed by Orner and Hartbower.[11] However, there seems to be a correlation between the two tests related to the processing conditions. A family of lines drawn approximately parallel to the 1:1 correlation line pass through the data points for materials with the same strain history. The unstrained materials lie on one such line, those strained at high temperature lie on another, etc. This suggests that the yield and/or strain hardening behavior resulting from each type of prior-strain history produces the observed effect. Further support of this is seen in Fig. 9 where the average yield strength for each group of data is plotted. It is seen that as the yield strength increases, the deviation from the 1:1 correlation becomes greater. An explanation of this in terms of the gross mechanical behavior at the crack tip is hypothesized.

In Table AII, the displacement gage results as well as the standard K_c data indicate that the plastic zone size remains relatively constant even with increasing yield strength. If the plastic zone size remains almost constant, the plastic energy absorption will be a function of σ_{ys}^2/E. In the small pre-cracked Charpy tests where the plastic zone is limited and the total plastic energy absorption relatively small, this effect may be masked. However, in the wide-plate tests where the plastic zone may fully develop, this effect may be strong. As the yield strength becomes larger, then, the gross deviation between the two tests becomes larger. It should be emphasized, however, that this is only the case for the rare instance where the plastic zone size at instability remains relatively constant with increasing strength. Thus, not only do the materials group according to thermal-mechanical treatment, but they also group according to yield strength level.

d. Structural Observations

The mechanical properties of the quenched and tempered and ausform steels varied systematically with processing conditions. There are undoubtedly structural changes accompanying this variation in properties. However, it was anticipated that with the small strains and low temperatures

employed, these changes would be on a fine scale. The initial structures were examined by light microscopy while the changes due to processing were examined by electron microscopy.

Light micrographs of the as-received ausform steels, Fig. 10, show a large amount of an isothermal decomposition product believed to be ferrite. It is known that ferrite produced during ausforming is detrimental to properties. Apparently this occurred in our materials since the strength and toughness were about ten percent below those previously reported.[4]

Extraction replicas were made of the quenched and tempered and ausform steels in several conditions. After strain aging, both materials exhibited a new dispersion, in addition to the cementite seen in the unstrained structures, as shown in Figs. 11 and 12. This dispersion was observed for all straining temperatures, but was especially evident after the 225° and 300°C treatments. The particle size was generally in the in the several hundred Angstrom range, and the morphology was similar in all steels. Attempts to identify the particles by electron diffraction have been inconclusive. This is not surprising considering the non-equilibrium conditions under which the carbides were formed. Such conditions are likely to lead to non-stoichiometry, and in some cases, to altered structures.

A few thin foils were prepared in order to obtain more information about the actual distribution of the particles. The structure of quenched and tempered Hy-Tuf after strain aging is shown in Fig. 13. The dispersoid seen in the replicas is best observed in thin foils by using bright and dark field illumination. Particles which appear dark in normal illumination become bright when one of their diffracted beams is used to form a dark field image.

The observed particle spacings are too large to account for the strength by an Orowan-type mechanism. The role of these particles in the strain aged steel may be similar to that of alloy carbides formed during ausforming. Thomas et al[14] suggest that the carbides act both as dislocation sources and as barriers, effectively increasing the dislocation density. Keh and Leslie[15] have observed in iron carbon alloys that dynamic strain aging produces a finer carbide dispersion and a higher dislocation density than either quench aging or static strain aging. Thus, the primary strengthening mechanism in dynamic strain aging may be that of increased dislocation density rather than dispersion hardening. These preliminary observations are being supplemented by thin foil studies of dynamically strain aged steels with and without alloy carbide forming elements.

SUMMARY AND CONCLUSIONS

The response of alloy steels to dynamic strain aging in both quenched and tempered and ausformed conditions was investigated. Strength, ductility, and toughness were measured as a function of straining and tempering temperatures. Structural observations were made on the strained and unstrained steels. The results may be summarized as follows:

(1) All quenched and tempered steels strained at temperatures between 150° and 375°C exhibited stable stress-strain curves when subsequently tested at room temperature. In two of the ausform steels, either an instability or a limited work-hardening range was encountered with several processing conditions. This resulted in no observable effect on the fracture toughness.

(2) By appropriate choice of strain and tempering temperatures, the strength of quenched and tempered steels was increased by about 40,000 psi, i.e., to the base strength of the ausform steels. The strength of the ausform steels was increased by about the same amount, suggesting that the strengthening effects are additive.

(3) At the same yield strength, the toughness of the quenched, tempered and strain aged steels, as measured by the pre-cracked Charpy test (high strain rate) is significantly greater than that of the ausform steels in the unstrained condition. This superiority of the quenched and tempered steels may be related to the presence of an isothermal decomposition product in the ausform steel.

(4) The correlation between pre-cracked Charpy and wide-plate fracture toughness tests is dependent upon prior strain history and yield strength level. A tentative explanation of this based upon the plastic energy absorption in each type of specimen is given.

(5) The observed variation of toughness with strain temperature suggests that room temperature strain aging be investigated in both ausform and quenched and tempered steels.

(6) Preliminary structural studies indicate that a new carbide dispersion is produced by dynamic strain aging. As yet, this carbide has not been identified.

(7) In the ausform steels, yield strengths of 270,000 psi were achieved by dynamic strain aging with a reliability ratio (K_c/σ_{ys}) of one. Since the slope of K_c/σ_{ys} vs σ_{ys} is small, it is suggested that this process may be used to attain yield strengths of 300,000 psi with exceptional toughness.

ACKNOWLEDGEMENTS

The authors are indebted to the Crucible Steel Company for undertaking the difficult task of ausforming these low alloy steels. Also, they wish to thank Messrs. R. Nickerson, K. V. Ravi, and D. Fahr for their enthusiastic assistance in several aspects of this project. Finally, discussions with Professor G. Thomas of the University of California were most helpful.

This work was performed under the auspices of the United States Atomic Energy Commission.

REFERENCES

1. Fracture Testing of High-Strength Sheet Materials, A Report of a Special ASTM Committee, ASTM Bulletin, January and February, 1960.
2. W. W. Gerberich, ASM Met. Eng. Quart., 5, No. 4, 1964.
3. R. F. Decker, J. T. Eash and A. J. Goldman, Trans. ASM, 55, 1962.
4. W. W. Gerberich, A. J. Williams, C. F. Martin and R. E. Heise, "Structure and Properties of Ultra High-Strength Steels", ASTM Spec. Tech. Pub. 370, Baltimore, 1965.
5. A. B. Smith, ASM Met. Eng. Quart., 3, No. 4, 1963.
6. W. W. Gerberich, W. G. Reuter and L. Raymond, "On the Structure Sensitivity of Fracture Toughness", submitted for publication.
7. W. W. Gerberich, unpublished results.
8. V. S. Goel, "Elevated Temperature Strain Aging of Conventional and Ausform Steels", Ph. D. Thesis, University of California, Berkeley, January, 1965.
9. E. T. Stephenson and M. Cohen, Trans. ASM 54, 1961, p. 72.
10. C. C. Busby, M. F. Hawkes, H. W. Paxton, and R. F. Mehl, "Flow and Fracture Characteristics of Low Carbon Martensites", WADC Technical Report, 53-517, February, 1954.
11. G. M. Orner and C. E. Hartbower, Welding Journal Res. Suppl., September, 1961.
12. F. A. McClintock and G. R. Irwin, ASTM Symposium on Crack Toughness Testing and Applications, June, 1964.
13. J. L. Swedlow and W. W. Gerberich, Proc. Soc. for Exp. Stress Anal., 1964.
14. G. Thomas D. Schmatz and W. W. Gerberich, High Strength Materials, V. F. Zackay, Editor. J. Wiley and Sons, New York, 1965, p. 251.
15. A. S. Keh and W. C. Leslie, "Structure and Properties of Engineering Materials", H. H. Stadelmaier, Editor. Interscience, New York, 1964, p. 208.

Table 1. Compositions of the Steels Investigated

	C	Cr	Mo	V	Ni	Mn	Si
HY TUF	0.25	0.30	0.39	—	1.74	1.35	1.25
D6AC	0.26	1.14	0.99	0.02	0.54	0.70	0.22
5M21	0.19	0.48	2.93	—	3.02	0.49	0.36

Appendix Tables

TABLE AI: MECHANICAL PROPERTY DATA

Material[1] & Condition	Yield Strength σ_{ys}, ksi	Tensile Strength σ_{ts}, ksi	Elongation % in 1.4"	Toughness[2] in-lb/in^2	Type of[3] Stress Strain Curve
HA-11	273	277	2.9	928	II
12	273	276	2.9	1171	II
13	272	272	2.8	1127	II
14	254	255	3.7	1220	II
22	244	261	4.3	1232	I
23	257	263	4.3	1261	I
24	233	243	3.6	1268	I
33	265	267	4.3	1407	II
34	246	246	3.6	1449	Brittle
44	242	244	3.6	1511	II
HAX-22	221	257	5.0	1584	I
HQ-11	197	230	6.4	2582	I
12	198	227	5.7	1864	I
13	214	226	5.7	1900	I
14	210	226	5.7	2043	I
22	219	238	5.7	1605	I
23	232	246	6.4	1780	I
24	221	238	5.0	1998	I
33	224	229	4.3	1594	I
34	219	221	5.0	1726	I
44	227	231	4.3	1066	I
HQX-22	186	220	7.1	1881	I
DA-11	---	282	2.9	379	Brittle
12	---	276	2.9	432	Brittle
13	---	286	2.9	488	Brittle
14	269	270	2.1	504	III
22	266	266	2.9	939	III
23	270	270	2.9	881	III
24	---	252	---	853	III
33	248	260	5.0	1104	I
34	234	243	5.0	1190	I
44	234	241	5.0	1047	I
DAX-22	226	265	5.7	1467	I
DQ-11	192	221	7.1	1978	I
12	191	217	5.0	1756	I
13	192	210	6.4	1738	I
14	193	215	6.4	1835	I
22	217	229	4.3	1741	I
23	203	222	5.0	1407	I
24	194	212	5.7	1450	I

TABLE AI (Cont.)

Material[1] & Condition	Yield Strength σ_{ys}, ksi	Tensile Strength σ_{ts}, ksi	Elongation % in 1.4"	Toughness[2] in-lb/in^2	Type of[3] Stress Strain Curve
DQ-33	216	223	3.6	1356	I
34	205	212	4.3	1372	I
44	207	216	5.0	1246	I
DQX-22	190	217	5.0	2043	I
MA-11	267	280	5.0	1052	I
12	267	276	3.6	1020	I
13	257	269	5.0	872	I
14	243	252	5.7	904	I
22	235	253	5.0	1132	I
23	220	244	5.0	1001	I
24	221	235	6.4	971	I
33	247	263	4.3	916	I
34	232	251	5.0	866	I
44	229	245	5.7	847	I
MAX-22	212	256	6.4	1121	I
MQ-11	176	214	7.1	1910	I
12	185	211	7.1	1746	I
13	181	206	7.1	1457	I
14	186	209	6.4	1431	I
22	200	209	5.7	1828	I
23	193	206	6.4	1747	I
24	190	202	6.4	1678	I
33	209	219	4.3	1152	I
34	196	208	5.0	1511	I
44	171	176	7.1	1203	I
MQX-11	170	212	7.1	2236	I
22	172	216	7.1	1966	I

(1) Material Designation: M(5M21); D(D6aC); H(Hy-Tuf); A(Ausform); Q(Quenched & Tempered); X(Unstrained). Numbers refer to strain and tempering temperatures, respectively (150, 225, 300, 375°C).

(2) From Pre-Cracked Charpy Tests.

(3) See Section Entitled "Shape of Stress-Strain Curve".

TABLE AII: WIDE PLATE FRACTURE TOUGHNESS DATA

Material & Condition (1)	Plate Dimension, Inches Width	Thick	Yield Strength, σ_{ys}, ksi	Ultimate Strength, σ_{ts}, ksi	Applied Stress, σ_o, ksi	Critical Crack (2) 2a, in.
MAX-12	5.15	0.064	211.6	256.3	101.5	2.15
MA-11	5.15	0.064	266.6	280.0	118	2.15
MA-11	5.15	0.062	266.6	280.0	124.5	2.14
MA-23	5.15	0.0595	220.2	244.4	107.5	2.22
MA-23	5.16	0.063	220.2	244.4	113	2.01
MA-33	4.68	0.062	246.8	262.7	105.5	1.975
MA-33	4.69	0.058	246.8	262.7	110.5	2.13
DAX-12	5.15	0.060	226.3	265.4	108	2.175
DA-14	4.69	0.065	269.2	269.6	123	2.15
DA-14	4.69	0.062	269.2	269.6	126	2.05
DA-22	5.15	0.059	266.3	266.3	119	2.15
DA-22	5.15	0.0575	266.3	266.3	113.5	2.03
DA-33	4.68	0.0595	247.9	259.8	119	2.015
DA-33	4.69	0.058	247.9	259.8	106	1.90
HAX-12	4.68	0.058	221.0	256.8	110.5	2.06
HA-11	4.68	0.0585	272.8	277.0	115	2.09
HA-11	4.69	0.065	272.8	277.0	132.5	2.065
HA-23	4.68	0.061	256.7	263.3	> 113 (7)	----
HA-23	4.68	0.058	256.7	263.3	124	1.90
HA-33	4.69	0.060	264.6	267.0	113	1.93
HA-33	4.69	0.060	264.6	267.0	112	2.20

TABLE AII (continued)

Material & Condition(1)	Effective (3) Crack 2a', in.	Fracture (4) Toughness K_c, ksi$\sqrt{in.}$	Fracture (5) Toughness K_c, ksi$\sqrt{in.}$	G_c (4) in-lb/in^2	G_c (5) in-lb/in^2
MAX-12	3.25	226	284	1700	2660
MA-11	3.09	257	314	2200	3260
MA-11	----(6)	274	---	2500	----
MA-23	3.29	247	305	2030	3100
MA-23	2.90	244	286	1980	2720
MA-33	----(6)	221	---	1620	----
MA-33	2.92	246	291	2000	2800
DAX-12	3.35	239	312	1900	3230
DA-14	----(6)	277	---	2540	----
DA-14	3.14	276	359	2530	4260
DA-22	2.93	260	303	2260	3060
DA-22	----(6)	234	---	1820	----
DA-33	----(6)	258	---	2230	----
DA-33	2.69	214	257	1520	2200
HAX-12	2.82	246	281	2000	2640
HA-11	2.82	250	293	2080	2840
HA-11	3.16	292	381	2830	4800
HA-23	----	---	---	----	----
HA-23	2.58	259	292	2240	2840
HA-33	2.53	230	262	1770	2280
HA-33	2.89	253	294	2130	2860

(1) See Table AI for Condition Designation

(2) From Ink Measurement

(3) From Displacement Gage

(4) From 2a Measurement Using Equation 1

(5) From 2a' Measurement Using Equation 2

(6) Displacement Gage Malfunction

(7) Doubler Broke

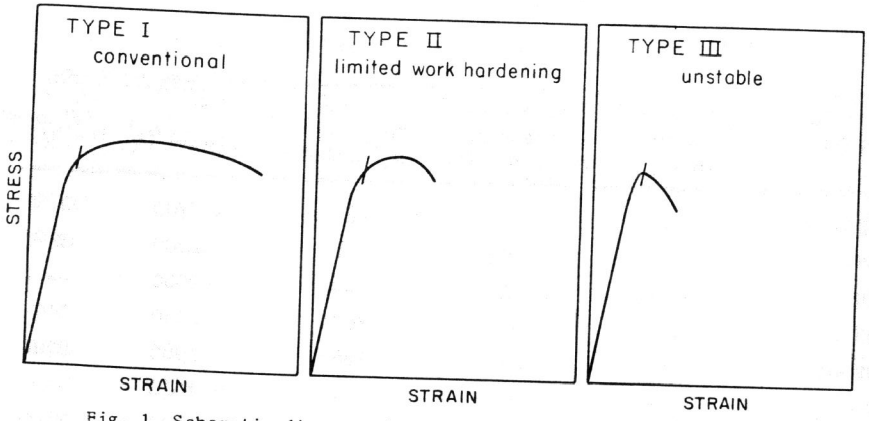

Fig. 1 Schematic diagram of the types of stress-strain curves observed.

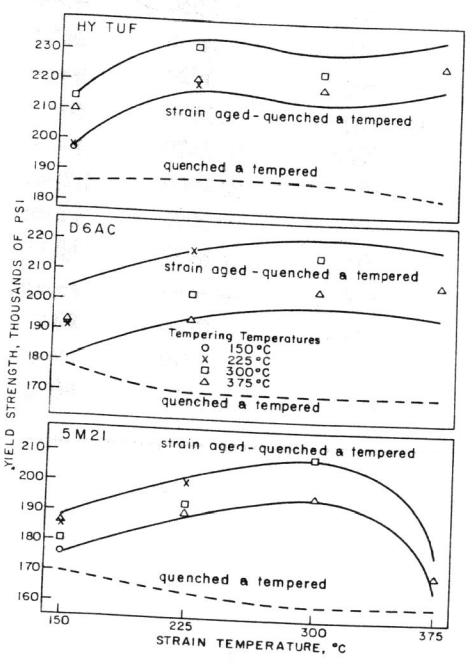

Fig. 2 The yield strength as a function of strain temperature for several tempering temperatures for the quenched and tempered steels.

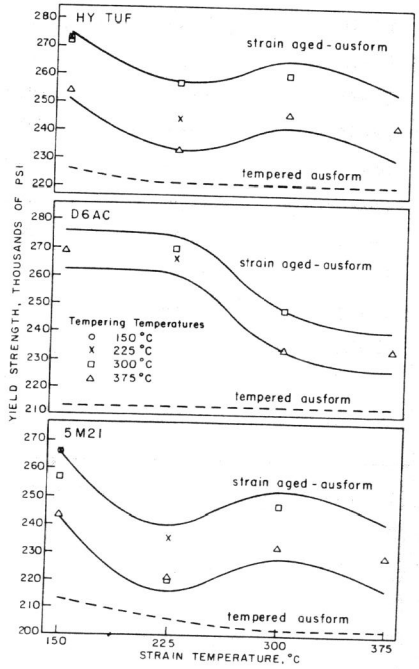

Fig. 3 The yield strength as a function of strain temperature for several tempering temperatures for the ausform steels.

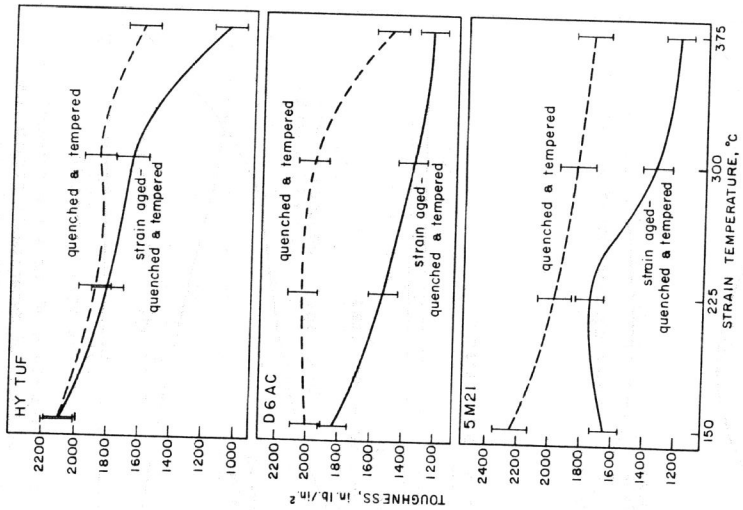

Fig. 5 The toughness as a function of strain temperature for the quenched and tempered steels.

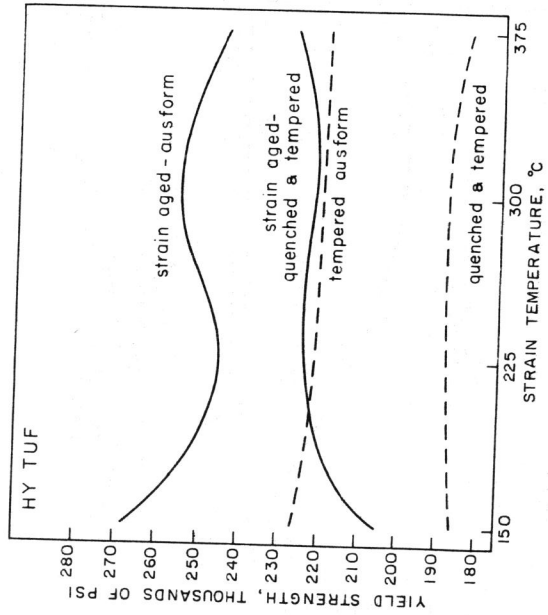

Fig. 4 A comparison of the yield strengths of dynamically strain aged quenched and tempered and ausform Hy-Tuf as a function of strain temperature.

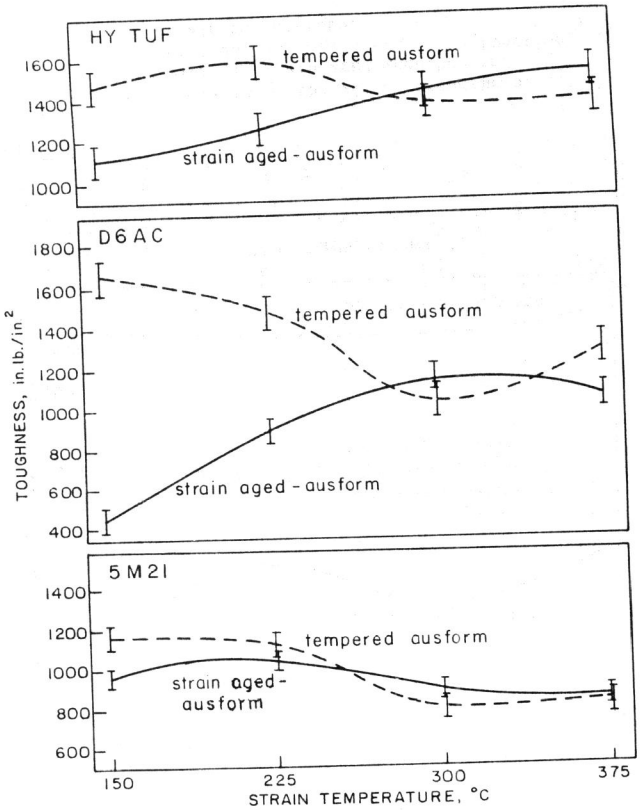

Fig. 6 The toughness as a function of strain temperature for the ausform steels.

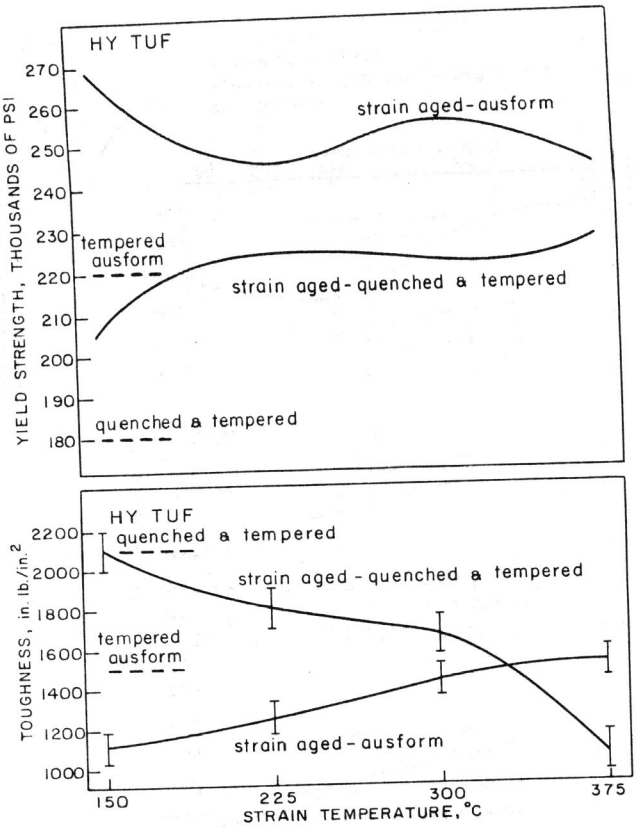

Fig. 7 A comparison of the yield strength and toughness of dynamically strain aged quenched and tempered and ausform Hy-Tuf.

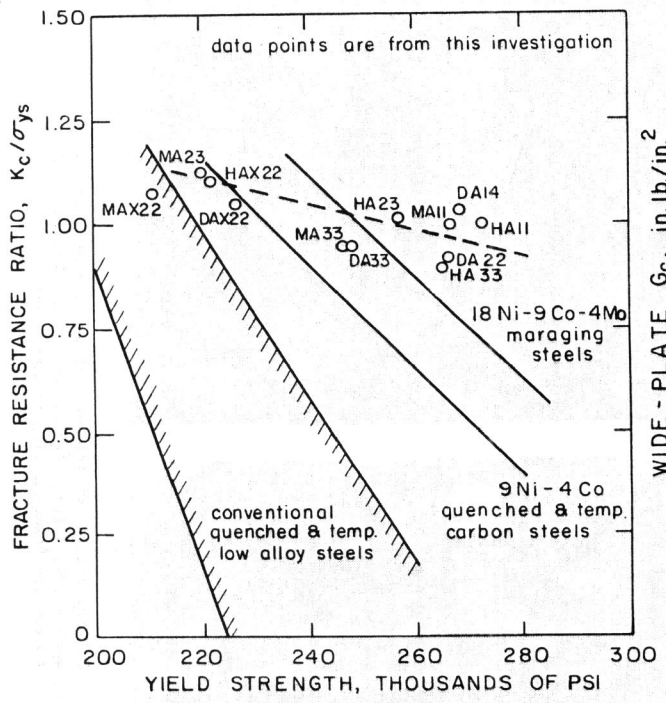

Fig. 8 Fracture resistance ratio (K_c/σ_{ys}) versus yield strength for the best commercially available ultra-high strength steels. Data points are from this investigation.

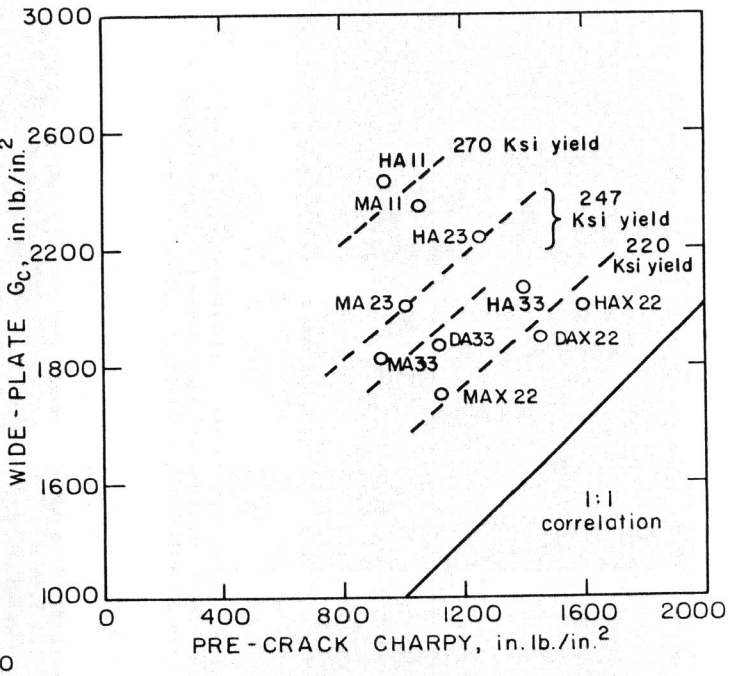

Fig. 9 Wide plate toughness (obtained from $G_c = K_c^2/E$) vs pre-cracked Charpy toughness for ausform steels. "X" designates the unstrained condition; the two digits refer to strain and tempering temperatures, respectively, (1-150°C, 2-225°C, 3-300°C), and M, H, and D refer to 5M21, Hy-Tuf, and D6aC.

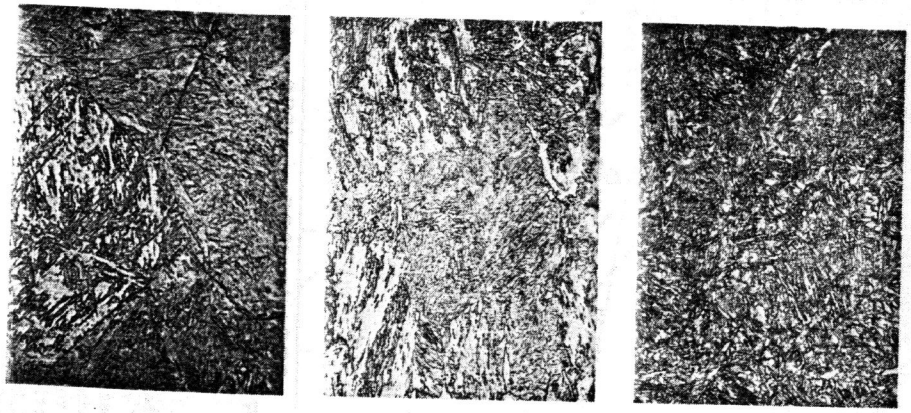

Fig. 10 Optical micrographs of the as-received ausform steels: left-5M21; middle-Hy-Tuf; right-D6aC. The light etching areas are believed to be ferrite. Etched in nital.

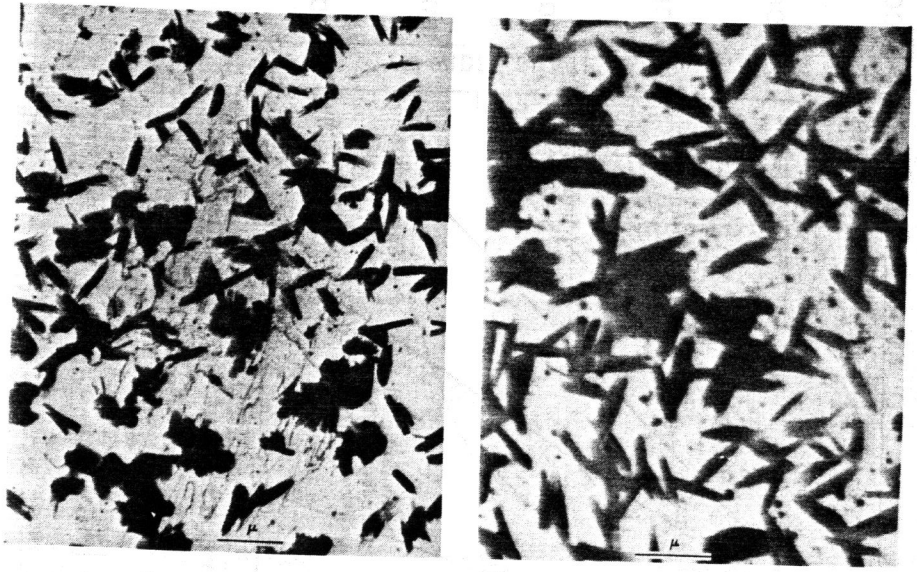

Fig. 11 Carbide extraction replicas of ausform Hy-Tuf: left-unstrained; right-strained at 300°C. The small particles are formed during strain aging.

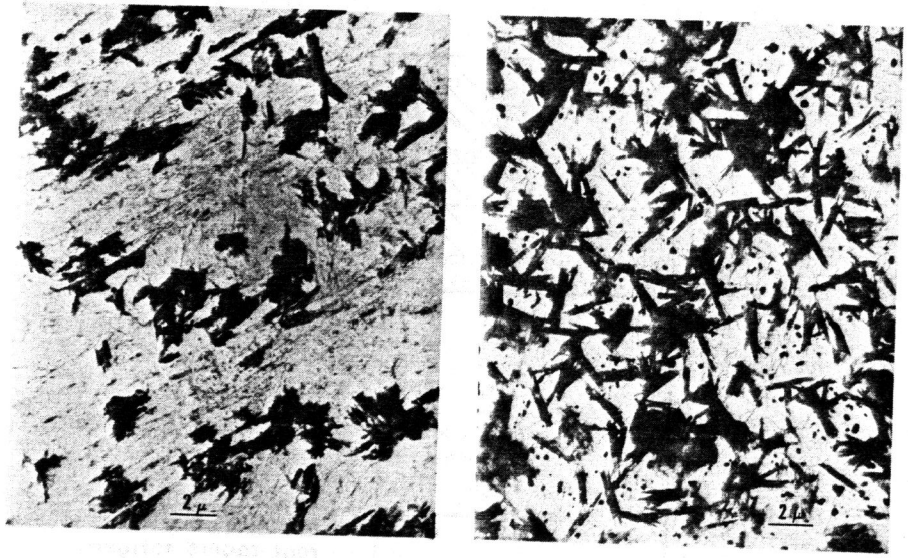

Fig. 12 Carbide extraction replicas of ausform D6aC: left-unstrained; right-strained at 225°C.

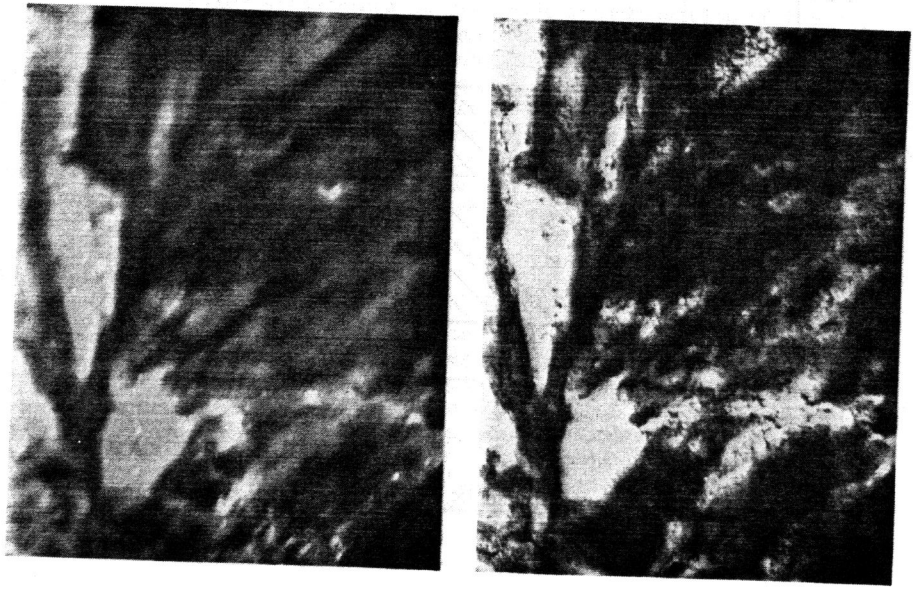

Fig. 13 Transmission micrograph of strain aged quenched and tempered Hy-Tuf. The small particles are observed to reverse contrast in dark field.

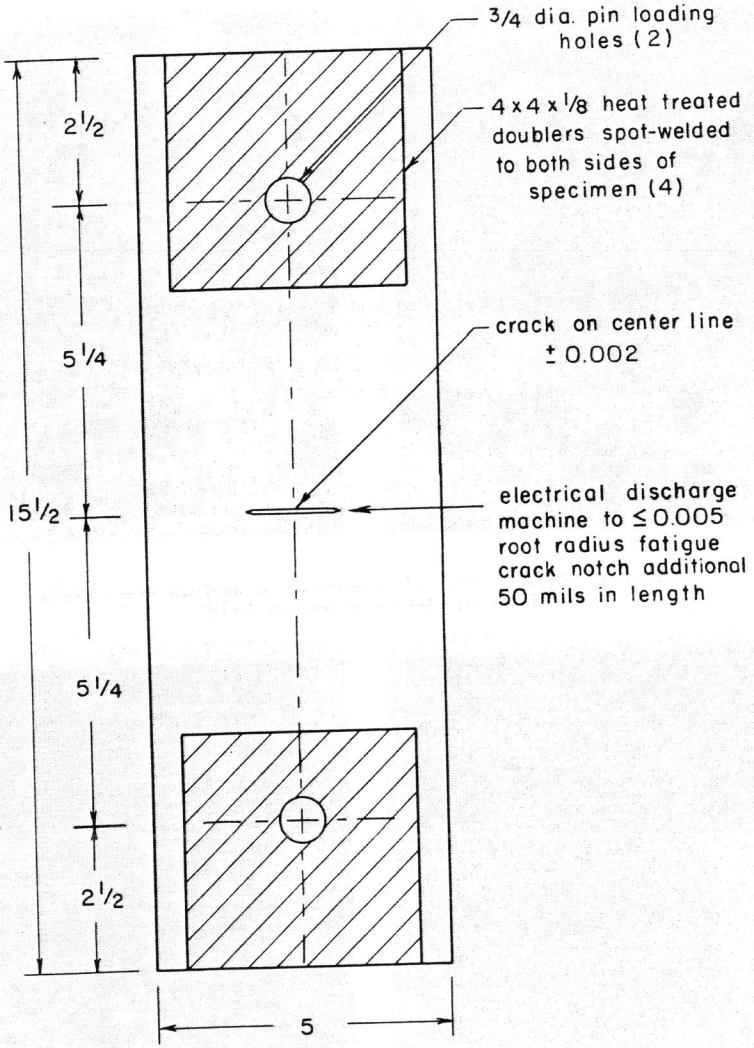

Appendix Figure

Fig. AI Dimension wide plate fracture toughness specimen.